

A Dual-Enzyme Amplification Loop for the Sensitive Biosensing of Endopeptidases

Chuanwen Zhou, Xiaomin Li, Sze Wing Tang, Chunxi Liu, Michael H. W. Lam,* and Yun Wah Lam*

Cite This: *ACS Omega* 2023, 8, 25592–25600

Read Online

ACCESS |



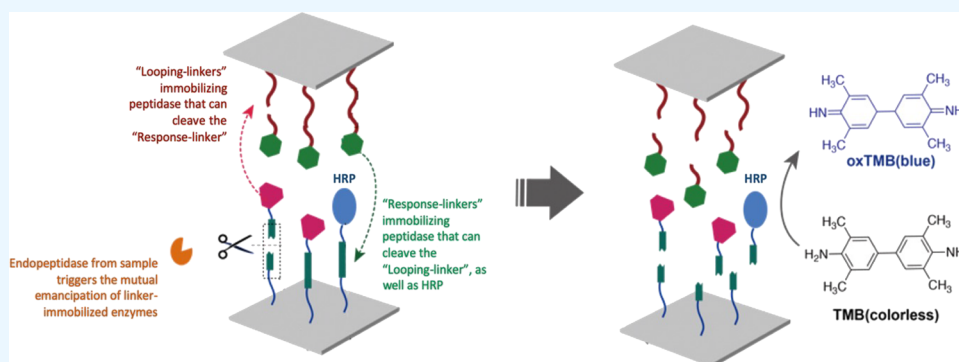
Metrics & More



Article Recommendations



Supporting Information



ABSTRACT: A rapid and sensitive approach for the detection of endopeptidases via a new analyte-triggered mutual emancipation of linker-immobilized enzymes (AMELIE) mechanism has been developed and demonstrated using a matrix metalloproteinase, a collagenase, as the model endopeptidase analyte. AMELIE involves an autocatalytic loop created by a pair of selected enzymes immobilized on solid substrates via linkers with specific sites that can be proteolyzed by one another. These bound enzymes are spatially separated so that they cannot act upon their corresponding substrates until the introduction of the target endopeptidase analyte that can also cleave one of the linkers. This triggers the self-sustained loop of enzymatic activities to emancipate all the immobilized enzymes. In this proof of concept, signal transduction was achieved by a colorimetric horseradish peroxidase–tetramethylbenzidine (HRP–TMB–H₂O₂) reaction with HRP that are also being immobilized by one of the linkers. The pair of immobilized enzymes were collagenase and alginate lyase, and they were immobilized by an alginate linker and a short peptide chain containing the amino acid sequence of Leu-Gly-Pro-Ala for collagenase. A detection limit of 2.5 pg collagenase mL⁻¹ with a wide linear range up to 4 orders of magnitude was achieved. The AMELIE biosensor can detect extracellular collagenase in the supernatant of various bacteria cultures, with a sensitivity as low as 10³ cfu mL⁻¹ of *E. coli*. AMELIE can readily be adapted to provide the sensitive detection of other endopeptidases.

INTRODUCTION

The use of molecular sensors for the screening of target analytes is an attractive concept for point-of-care diagnostics, environmental and food safety surveillance, security and counterterrorism, product safety/quality compliance monitoring, and many other real-world applications. They supplement advanced instrumental analytical and bioanalytical measurements with their characteristics of easy to use, rapid responses, high portability, and low operational cost.^{1–4} As more and more advanced applications of molecular sensors are calling for ever increasing detection sensitivity, various mechanisms that enable the generation of multiple signals from every single analyte–receptor binding event have drawn the attention of the chemo- and biosensing research communities in the recent decade.⁵ Perhaps, enzyme-linked immunosorbent assays (ELISA) were among the earliest examples of biosensing technology that harnessed the catalytic properties of enzyme-tagged antigen/antibody for signal amplification.⁶ Other

elegant mechanisms that involve the use of DNA aptamers,^{7–9} cascaded enzymatic reactions,^{10,11} generation/unmasking of molecular catalysts or catalytic surfaces on nanoparticles,^{12–14} dendritic chain reactions,^{15–19} and so forth, with electrochemical or colorimetric/fluorometric signal transduction, have also been explored. Nevertheless, new techniques that allow lower production/operational cost, more sensitive detection, faster responses, and more user-friendliness are still in demand.

Peptidases, enzymes that catalyze proteolysis, are essential to a wide variety of physiological processes for normal cellular

Received: May 24, 2023

Accepted: June 23, 2023

Published: July 7, 2023



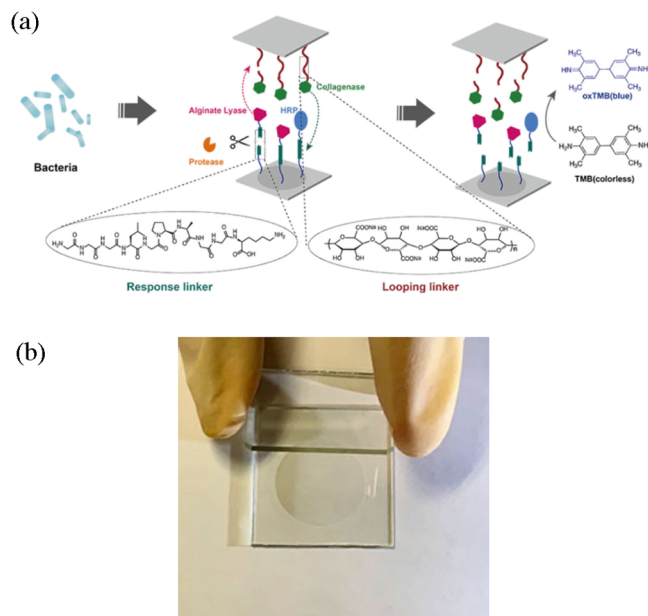
and tissue functioning such as the regulation of intracellular signal transduction and protein–peptide transportation, digestion, reproduction, innate immune responses, wound healing, and so forth. They are also involved in cancer cell proliferation and angiogenesis.^{20–23} Some extracellular peptidases of pathogens are known virulence factors.^{24–26} Their potentials as biomarkers for disease diagnostics and as drug targets for therapies are being increasingly recognized in recent years.^{27–30} Traditional assays for peptidases such as gel zymography^{31,32} and antibody-based immunoassays^{33,34} are usually slow, tedious, and costly. Numerous approaches for the biosensing of peptidases making use of their specific peptide cleaving properties to induce luminescence or electrochemical responses have been developed in recent years.^{35–37} Detection sensitivity can be further enhanced by coupling peptide cleavage to DNA aptamer-based amplification strategies^{38,39} or cascaded enzymatic reactions.^{40–42}

In this work, we explore the feasibility of a new signal amplification approach for the sensitive screening of endopeptidases capable of producing rapid colorimetric responses readily detectable by the naked eye. This analyte-triggered mutual emancipation of linker-immobilized enzymes (AMELIE) strategy enables the generation of multiple signals from a single molecular recognition event using a pair of bound enzymes immobilized by linkers that are proteolytic substrates of one another. One of the linkers, the “response-linker” contains the specific peptide sequence that can be selectively cleaved by the target endopeptidase analyte. The other linker, the “looping-linker”, is composed of the substrate for the enzyme immobilized by the response-linkers. It is responsible for the controlled release of the other member of the dual-enzyme pair that can also cleave the response-linkers, spawning a self-sustained, autocatalytic loop of enzymatic reactions leading to the emancipation of all the bound enzymes. Colorimetric responses are generated by a horseradish peroxidase–tetramethylbenzidine (HRP–TMB) system where the HRP is also immobilized by the response-linker (Scheme 1). Spatial separation of these bound enzymes prevents the mutual proteolysis reactions from occurring in the absence of the target analyte, which upsets many other signal amplification mechanisms in chemo-/biosensing.⁴³ To demonstrate this concept, we constructed a biosensor for the detection of collagenase, a zinc-dependent matrix metalloproteinase (MMP). The signal amplifying autocatalytic loop was constructed from the immobilization of alginate lyase and collagenase by a peptide containing the Leu-Gly-Pro-Ala sequence specific for the target MMP as the response-linker and alginate as the looping-linker.

RESULTS AND DISCUSSION

Construction of the AMELIE Biosensor. The AMELIE biosensor for collagenase was constructed from readily available microscopy slides, with a planar glass slide lying on the top of a cavity well glass slide (Scheme 1). The cavity well of the bottom slide, which held $\sim 30 \mu\text{L}$ of analyte sample, was lined with response-linker-immobilized alginate lyase and HRP, while the upper slide was lined with looping-linker-immobilized collagenase. The collagenase-sensitive sequence GGGLGPAGGK on the response-linkers was adopted from the literature report of selective endopeptidase-degradable biomaterials by West and co-workers.^{45,46} Both ends of the peptide were conjugated to polyethylene glycol (PEG)–aldehyde chains via a Schiff base reaction for immobilization

Scheme 1. Design of the AMELIE Biosensor for the Detection of Collagenase: (a) Configuration of the Biosensor and a Brief Outline of the AMELIE Mechanism; (b) Biosensor Prototype Composed of Two Glass Slides Immobilized with the Dual-Enzyme System that Generates the Signal Amplifying Autocatalytic Loop



onto the γ -amino-propyl-trimethoxy silane (APTES)-treated glass substrate and the grafting of enzymes.^{47,48} The looping-linkers were constructed from partially oxidized alginate by NaIO_4 ⁴⁹ to provide the aldehyde functionalities for enzyme grafting and substrate immobilization. After being triggered by the analyte endopeptidase—collagenase, the response-linkers are proteolyzed to release alginate lyase, as well as HRP, from the bottom slide. The released alginate lyase diffuses to the upper slide, degrades the looping-linkers, and liberates more collagenase, which, in turn, diffuses to the lower slide to free more alginate lyase and HRP. Hence, this enzyme cascade system essentially amplifies the copy number of collagenase in the reaction, which released the immobilized HRP into solution. This autocatalytic loop will continue until all bound enzymes are released. The amount of unbound HRP is then detected by the signal generated from the catalyzed oxidation of TMB by H_2O_2 in the resulting solution.

Figure 1 shows the signals generated by the release of HRP initially immobilized via response-linker and looping-linker in various configurations. These devices were incubated with corresponding enzymes for 15 min, a treatment time that produced saturation signals for AMELIE (see Figure 2). HRP immobilized via the response-linker (collagenase substrate) and the looping-linker (alginate) could be detectably released by 10 pg mL^{-1} of collagenase (device a) and alginate lyase (device b), respectively.

Next, we examined devices with spatially separated linker-immobilized enzymes. One set of devices was composed of looping-linker-immobilized-collagenase and response-linker-immobilized-HRP (device c), and another set was of response-linker-immobilized-alginate lyase and looping-linker-immobilized-HRP (device d). These configurations allow for a two-step enzymatic release of HRP. For example, the introduction of alginate lyase (10 pg mL^{-1}) into the reaction

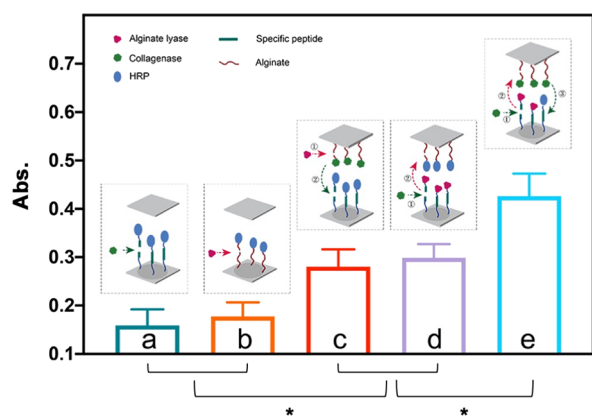


Figure 1. Colorimetric responses (in terms of absorbance at 450 nm) of the HRP-TMB-H₂O₂ reaction from the various devices: (a) collagenase + response-linker-immobilized-HRP; (b) alginate lyase + looping-linker-immobilized-HRP; (c) alginate lyase + looping-linker-immobilized-collagenase + response-linker-immobilized-HRP; (d) collagenase + response-linker-immobilized-alginate lyase + looping-linker-immobilized-HRP; (e) an AMELIE device. Error bars represent standard deviations of data sets with a sample size of 3 (**p* < 0.01).

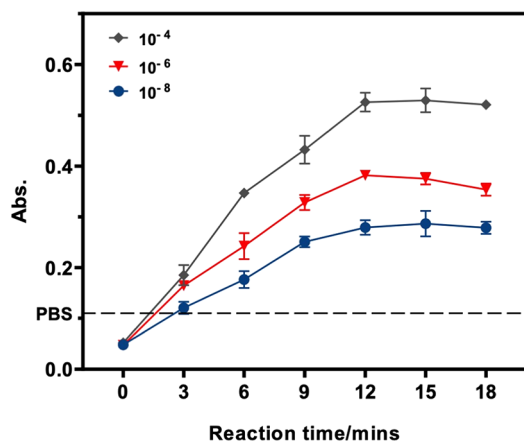


Figure 2. Time courses of AMELIE biosensor responses (in terms of absorbance at 450 nm) at analyte concentrations of 10, 10³, and 10⁵ pg collagenase mL⁻¹. Error bars represent standard deviations of data sets with a sample size of 3. The dotted line indicates the absorbance at the 15 min time point in the absence of collagenase (PBS control).

resulted in the cleavage of the alginate-linker to which collagenase was anchored. The liberated collagenase then cut the looping-linkers, releasing the immobilized HRP (device c). Colorimetric responses shown in bars c and d were significantly stronger than those for their corresponding solo linker devices (bars a and b). As the amounts of collagenase, alginate lyase, and HRP used in all devices were the same, these data indicate that HRP was released at a faster rate by the two-step enzymatic cleavage (bars c and d) than solo cleavage (bars a and b). Bar e shows the colorimetric response of a complete AMELIE design in which immobilized collagenase and alginate lyase were released in a positive feedback loop. We observed a ~9-fold increase in the release of HRP triggered by the same initial concentration of collagenase using the AMELIE reaction (device e) compared to single-step enzymatic cleavage (device a), suggesting that the dual-enzyme autocatalytic loop can effectively amplify the signal of an endopeptidase assay.

The effect of incubation time to the overall AMELIE biosensing responses was assessed at three different analyte concentrations. Signals generally reached a plateau at about 15 min (Figure 2). The incubation time for all subsequent biosensing experiments was fixed at 15 min.

Signal Amplification, Analyte Selectivity, and Stability. To evaluate how the signal amplification demonstrated in Figure 1 affects the sensitivity of collagenase activity assay, we compared the signal strength for collagenase detection with and without AMELIE. This was achieved by using a control device in which the upper coverslip of the AMELIE device depicted in Scheme 1a (i.e., device e in Figure 1) was replaced by a plain glass slide. In this control, the collagenase in the analyte could still release some immobilized HRP, but the amount of collagenase in the reaction was not amplified by the autocatalytic loop. As shown in Figure 3, the AMELIE

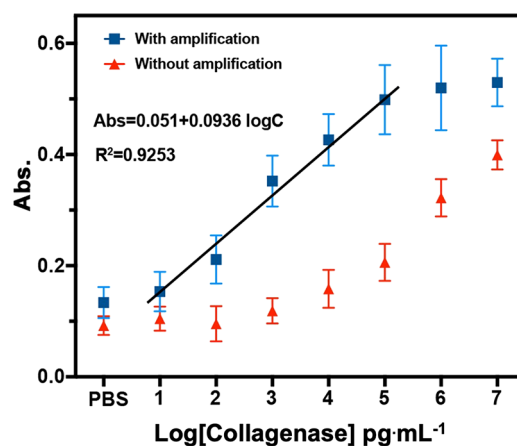


Figure 3. Signal intensity of the amplified and unamplified biosensor (in terms of absorbance at 450 nm) generated at different analyte concentrations from 1 to 10⁶ pg collagenase mL⁻¹ and response linearity over the range of analyte concentrations from 1 pg mL⁻¹ to 10 ng mL⁻¹.

biosensor produced significantly stronger sensing responses than the control throughout the concentration range of analyte adopted for evaluation. The plateauing of the biosensor response beyond 10 ng collagenase mL⁻¹ was likely due to the emancipation of all the bound HRP under the combined action of the analyte and the collagenase released from the degradation of the looping-linkers.

Figure 3 demonstrates the level of sensitivity enhancement of collagenase activity detection by AMELIE. Using AMELIE, the signal produced by collagenase at 1 ng mL⁻¹ (log 3 pg mL⁻¹) was similar to, if not slightly stronger than, that produced without AMELIE at 1000 ng mL⁻¹ (log 6 pg mL⁻¹). Similarly, the AMELIE signals at 10 and 100 (log 1 and log 2) pg collagenase mL⁻¹ were similar to those of the control at analyte concentrations of ~10 and 200 ng collagenase mL⁻¹ (log 4 and log 5 pg mL⁻¹). This indicates that, although the magnitude of signal amplification by AMELIE for a given collagenase concentration seldom exceeded 10 times, it was enough to increase the sensitivity of collagenase detection by ~1000-fold. Our data also show the dynamic range of the AMELIE biosensor, which responded linearly over a span of 4 orders of magnitude of analyte concentration (black line, Figure 3). The detection limit of the biosensor achieved at the current level of enzyme loading was estimated to be 2.5 pg collagenase mL⁻¹.

Besides its target collagenase, responses of the AMELIE biosensor toward other common endopeptidases, for example, thrombin, trypsin, and chymotrypsin, were measured (Figure 4a). Significant signals were only obtained from collagenase. The selectivity of the biosensor for collagenase was further demonstrated with the use of known collagenase inhibitor, 1,10-phenanthroline, which suppressed its biosensing response toward collagenase to a level similar to those of other nontarget endopeptidases. The biosensor also showed negligible response to bovine serum albumin.

One of the versatilities of the AMELIE biosensing approach is that signal amplification and detection sensitivity can be conveniently adjusted via the enzyme loading of the autocatalytic loop (that is, the amounts of enzymes immobilized via the two linkers). Understandably, the higher the loading of the two enzymes that constitute the loop, the greater will be the biosensing responses. This is demonstrated in Figure 4b. Devices fabricated from increasing concentration of enzymes in the immobilization step produced progressively greater colorimetric responses. Figure 4c shows the stability of AMELIE biosensors that have been stored at 4 °C for different durations. Although the level of biosensing response suffered some degree of decline in the initial stage of storage, it gradually settled after 7 days, and the biosensor still retained about 87% of response strength after 2 weeks of storage. From the depicted stability trend, the biosensor should be able to remain its function for more extended period of storage.

Data in Figure 3 suggest that AMELIE can increase the sensitivity of collagenase activity assay by up to 1000-fold. We confirmed this by directly detecting the amounts of collagenase released due to linker cleavage by gelatin zymography (Figure 5). A calibration experiment using purified collagenase indicated that gelatin zymography could not detect collagenase at a concentration lower than 10^4 pg mL⁻¹ (Figure 5a). However, with AMELIE, collagenase at a concentration as low as 10 pg mL⁻¹ could trigger the release of collagenase readily detectable by zymography (Figure 5b), suggesting that the autocatalytic loop in AMELIE can amplify the analyte amount by at least 10,000-fold.

Kinetic Modeling of the AMELIE Process. The signal amplification mechanism of AMELIE relies on the triggered emancipation of immobilized enzymes. To understand the kinetics of such a process, we assume that each of the three linker-cleavage reactions involved follows the standard Michaelis–Menten kinetics: where E_{sample} and $E_{\text{collagenase}}$ are



the concentrations of unbound collagenase (from the sample or from the cleavage of the looping-linkers), E_{alginase} is the concentration of unbound alginate lyase from the cleavage of

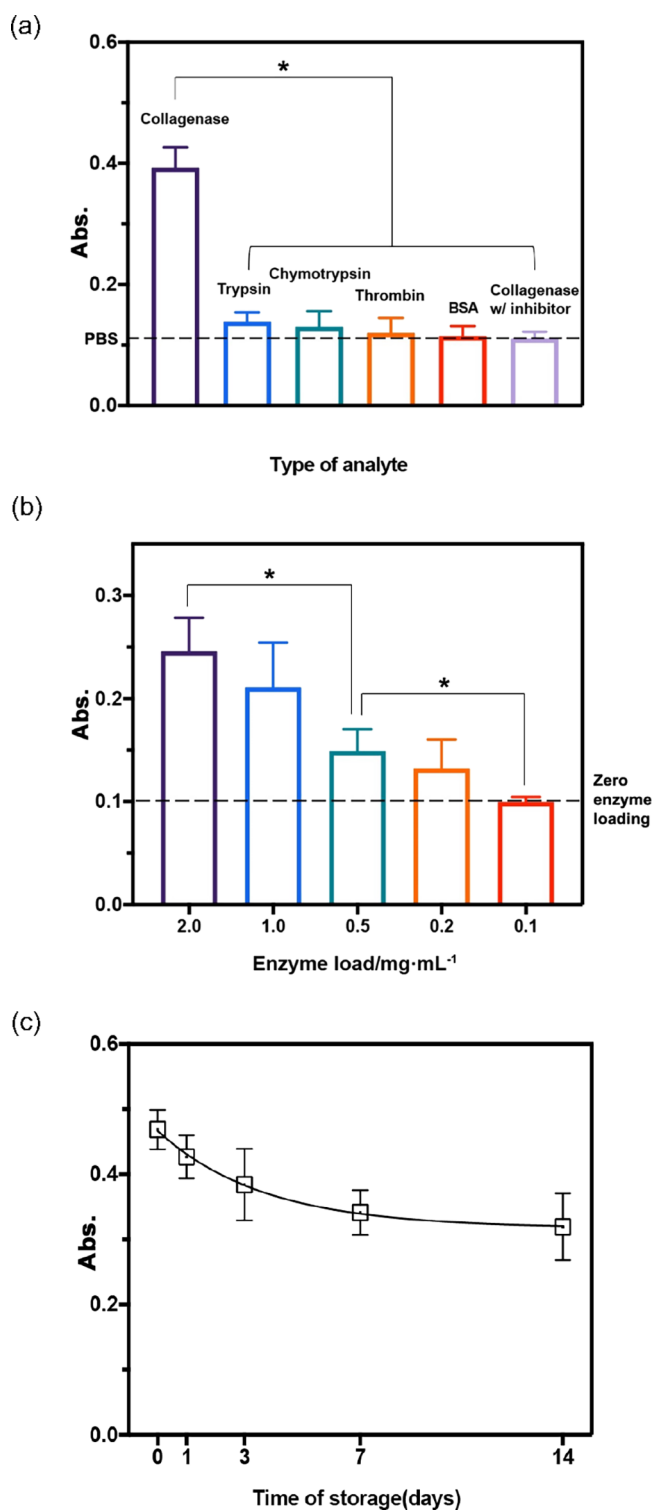


Figure 4. Performance of the AMELIE biosensor: (a) analyte specificity (concentration was 1 ng mL⁻¹ for all the endopeptidases; the inhibitor used was 1,10-phenanthroline). The dotted line represents the signal intensity in the absence of any enzyme. (**p* < 0.01); (b) biosensing responses at various enzyme loadings from 0.1 to 2 mg mL⁻¹, analyte concentration was 10 pg collagenase mL⁻¹. The dotted line represents the signal from the AMELIE device with no collagenase loading. (**p* < 0.05); (c) biosensor stability under 4 °C storage. Error bars represent standard deviations of data sets with a sample size of 3.

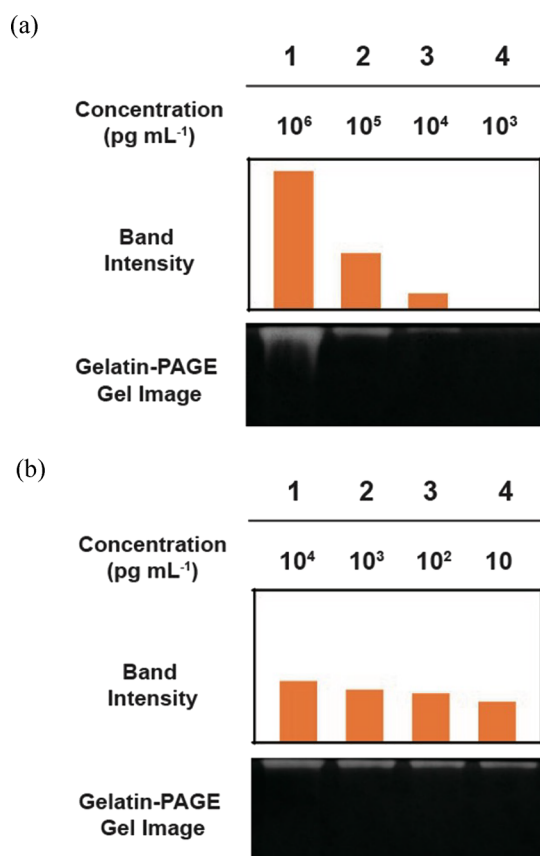


Figure 5. Signal amplification by AMELIE: (a) gelatin zymography of collagenase (10^3 to 10^6 pg mL^{-1}); (b) gelatin zymography of collagenase (10 to 10^4 pg mL^{-1}) after amplification by AMELIE.

the respond-linkers, E_{HRP} is the concentration of unbound HRP from the cleavage of the respond-linker, S_{respond} is the concentration of respond-linker bearing the linker-bound alginate lyase, S_{looping} is the concentration of looping-linker bearing the linker-bound collagenase, k_{cat1} is the conditional catalytic rate constant for the cleavage of the respond-linker by collagenase, and k_{cat2} is the conditional catalytic rate constant for the cleavage of the looping-linker by alginate lyase.

The rate of release of the linker-bound enzymes, ν , in the AMELIE biosensor at any time interval Δt becomes

$$\nu_{\text{alginate}} = \nu_{\text{HRP}} = \frac{k_{\text{cat1}} \cdot E_{\text{collagenase}} \cdot f \cdot S_{\text{respond}}}{K_{\text{M1}} + E_{\text{collagenase}}}$$

$$\nu_{\text{collagenase}} = \frac{k_{\text{cat2}} \cdot E_{\text{alginate}} \cdot f \cdot S_{\text{looping}}}{K_{\text{M2}} + E_{\text{alginate}}}$$

where ν_{alginate} is the rate of release of alginate lyase at the time interval Δt , $\nu_{\text{collagenase}}$ is the rate of release of collagenase at the time interval Δt , ν_{HRP} is the rate of release of HRP at the time interval Δt , f is the surface (A) to volume (V) ratio of the AMELIE biosensor ($A = 0.0314 \text{ dm}^2$, $V = 3 \text{ }\mu\text{L}$; $f = 10,467 \text{ dm}^{-1}$), k_{cat1} is the conditional catalytic rate constant for the cleavage of the respond-linker by collagenase, k_{cat2} is the conditional catalytic rate constant for the cleavage of the looping-linker by alginate lyase, K_{M1} is the conditional Michaelis constant for the formation of the $[E_{\text{sample}}S_{\text{respond}}]$ and $[E_{\text{collagenase}}S_{\text{respond}}]$ complex, and K_{M2} is the conditional

Michaelis constant for the formation of the $[E_{\text{alginate}}S_{\text{looping}}]$ complex.

A series of experiments were conducted using specially modified AMELIE devices with fluorescein isothiocyanate-labeled proteins (refer to the Supporting Information for details) to estimate the conditional kinetic parameters of the two enzymes involved in the AMELIE process. The approach developed by Gutiérrez et al.^{50,51} for heterogeneous enzymatic assays was adopted. From our measurements, k_{cat1} and K_{M1} of collagenase were 0.069 min^{-1} and 67.9 nM , respectively, while k_{cat2} and K_{M2} of alginate lyase were 0.0068 min^{-1} and 2.78 nM , respectively (Supporting Information).

The concentration of unbound enzymes, $[\text{collagenase}]_{\text{free}}$, $[\text{alginate lyase}]_{\text{free}}$, and $[\text{HRP}]_{\text{free}}$, in the aliquot of the AMELIE biosensor at any time t should be the cumulative amount of the enzymes released from their linkers:

$$[\text{collagenase}]_{\text{free}} = \sum_{t=0}^t \nu_{\text{collagenase}} \Delta t$$

$$[\text{alginate lyase}]_{\text{free}} = \sum_{t=0}^t \nu_{\text{alginate}} \Delta t$$

$$[\text{HRP}]_{\text{free}} = \sum_{t=0}^t \nu_{\text{HRP}} \Delta t$$

The output of the AMELIE biosensor is related to $[\text{HRP}]_{\text{free}}$. We found that under our experimental conditions, the extent of the HRP-TMB- H_2O_2 colorimetric responses was proportional to the concentration of the unbound HRP in the aliquot of the AMELIE biosensor. Figure 6 shows the result of a

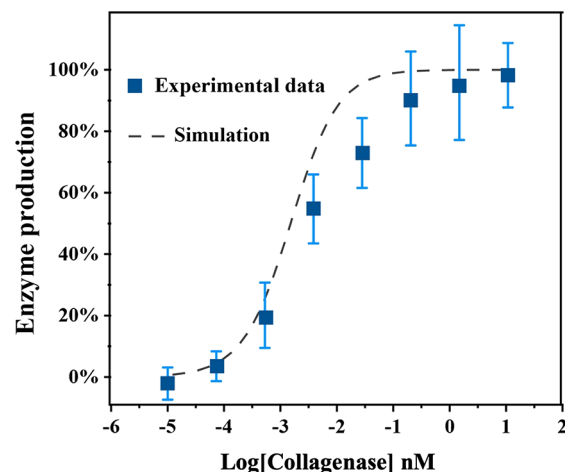


Figure 6. Levels of HRP released into the aliquot of AMELIE devices under different input concentrations of collagenase: simulation by kinetic model (dash line) versus experimental data (blue squares). The incubation time for all experiments was 15 min.

simulation by the above kinetic model for the AMELIE process. While the model is able to provide a reasonable account of the behavior of the AMELIE biosensor, it does not consider a number of factors. The examples of these factors, which are relatively difficult to be addressed, include (a) the nonuniformity of activity of the bound enzymes due to the various extents of structural change to their active sites that may be induced during the immobilization process and (b) the gradual deactivation of the enzymes involved in the

autocatalytic loop during the course of the AMELIE process. Works to refine the kinetic model to aid the selection of better dual-enzyme combination for more efficient AMELIE process are in progress.

Bacterial Biosensing. Bacteria are known to secrete proteolytic enzymes into the extracellular medium for them to obtain nutrients for energy production and resources for growth and reproduction.^{52,53} Some of the extracellular peptidases are also known virulence factors of pathogens.^{24–26,54} Thus, screening for the presence of specific extracellular peptidases in pathological and environmental samples can be useful for clinical diagnostics and food safety surveillance. We tested the AMELIE biosensor with five common bacterial pathogens, namely, *Serratia marcescens*, *Escherichia coli*, *Salmonella enterica*, *Staphylococcus aureus*, and *Pseudomonas aeruginosa*. All of them are known to produce extracellular collagenase. Figure 7a shows the responses of our AMELIE biosensor to their supernatants. These data also indicate that AMELIE worked in LB medium, a more complex, protein-rich matrix (1% milk-derived peptides and 0.5% yeast proteins) compared to inorganic buffer.

Next, we used *E. coli* for more in-depth evaluation of the performance of AMELIE biosensing for bacteria screening. Supernatants of *E. coli* cultures at various cell densities were applied onto the AMELIE biosensor. Figure 7b reveals that colorimetric responses significantly higher than that of the LB control could be obtained from supernatant of as low as 10^3 cfu mL^{-1} of *E. coli*, a titer within the clinically relevant range of *E. coli* in pathological samples.⁵⁵ Thus, AMELIE can potentially be developed as an ultrafast on-site detector of pathological bacteria.

Signal amplification by AMELIE was also verified by gelatin zymography. Direct detection of collagenase secreted by *E. coli* at 10^8 cfu mL^{-1} did not yield any detectable band (lane 1, Figure 7c). On the other hand, a strong band was obtained after the culture supernatant has gone through AMELIE amplification (lane 2, Figure 7c). Even after 10^4 times dilution, the AMELIE biosensor was still able to generate adequate collagenase in the aliquot to give an observable band (lane 4, Figure 7c).

CONCLUSIONS

This proof-of-concept work demonstrates the capability of the new AMELIE approach to detect endopeptidases with high sensitivity. The immobilization and spatial separation of enzymes by linkers that can respond to their enzymatic actions as well as that of the target endopeptidase analyte enable the generation of multiple signaling events from each analyte binding/interaction event for biosensing. This mechanism is different from the conventional cascaded catalytic/enzymatic reactions for signal amplification in chemosensing and biosensing and should significantly enhance the sensitivity of existing protease activity-based sensors.^{56,57} The extent of signal amplification can be conveniently toned by adjusting the loading of the immobilized enzymes and/or the surface dimensions of the biosensor. Analyte selectivity can be regulated by the substrate used in the response-linker. Thus, in theory, incorporation of suitable peptide sequence into the response-linker or substituting it with other substrates may afford AMELIE biosensors for other designated peptidases, hydrolases, lipases, and nucleases. As more than 100,000 cleavage specificities of over 4600 known proteases are currently known,⁵⁸ it is possible to select combinations of

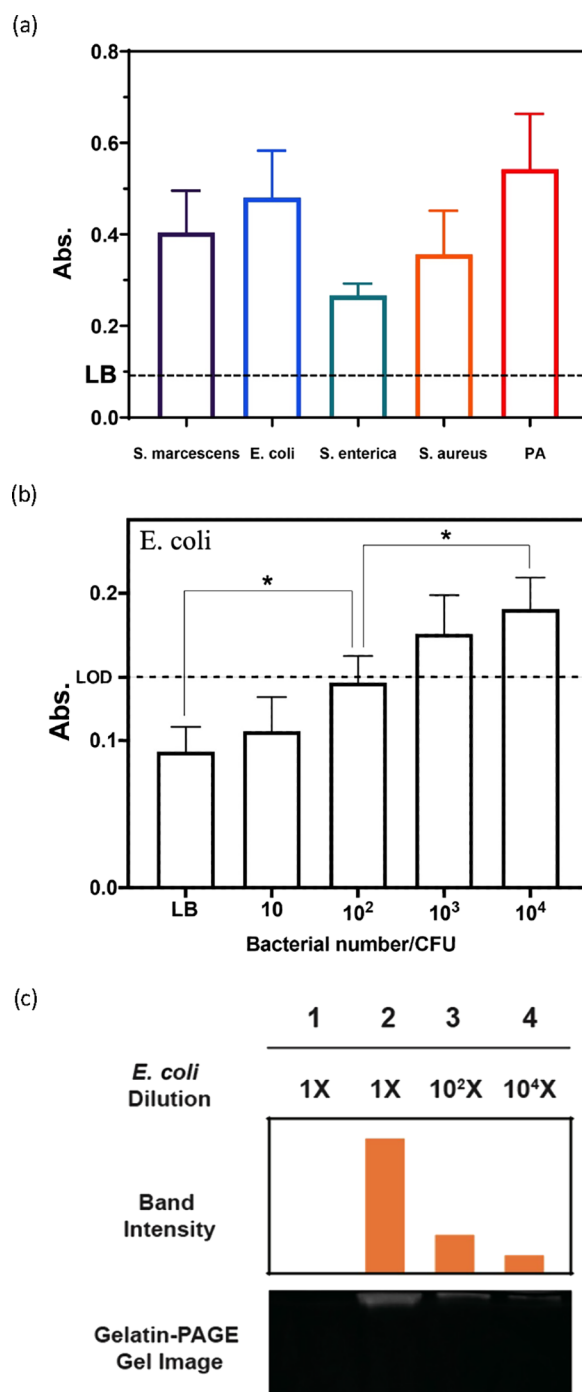


Figure 7. Application of the AMELIE process to bacterial biosensing: (a) responses of the AMELIE biosensor to supernatants of various bacteria cultures in LB broth at 10^8 cfu mL^{-1} . The dotted line represents the absorbance when no bacteria were used; (b) detection of collagenase in the supernatant of an *E. coli* culture. For (a) and (b), error bars represent standard deviations of data sets with a sample size of 3 ($*p < 0.01$); (c) gelatin zymograms of supernatants of *E. coli* cultures before and after AMELIE: lane 1, supernatant before AMELIE; lane 2, supernatant after AMELIE; lane 3, 10^2 times diluted supernatant after AMELIE; lane 4, 10^4 times diluted supernatant after AMELIE.

enzyme and linkers in AMELIE to circumvent the endogenous proteases and inhibitors associated with different matrices. Works on the development of AMELIE-based biosensors for bioanalytical applications are in progress.

EXPERIMENTAL SECTION

Materials and Apparatus. Collagenase from *Clostridium histolyticum* (Type I, ≥ 125 CDU mg^{-1} solid), alginate lyase ($\geq 10,000$ units/g solid), peroxidase from horseradish (HRP, Type VI, ≥ 250 units/mg solid), trypsin ($\geq 10,000$ BAEE units/mg protein), thrombin (lyophilized powder, 40–300 NIH units/mg protein), and chymotrypsin (Type II, lyophilized powder, ≥ 40 units/mg protein). 3,3',5,5'-Tetramethylbenzidine (TMB) liquid substrate system for ELISA, sodium alginate, LB broth, bovine serum albumin (BSA), and gelatin for electrophoresis were from Sigma-Aldrich, USA. Peptide sequence ($\text{H}_2\text{N-GGGLGPAGGK-OH}$) was synthesized and purified by Synpeptide Co. Ltd., China. Phosphate-buffered saline (PBS, pH 7.4) and cellulose dialysis tubing were from Gibco, Thermo Fisher Scientific, USA. Sodium periodate (NaIO_4), sodium cyanoborohydride (NaBH_3CN), dimethyl sulfoxide (DMSO), and γ -amino-propyl-trimethoxy silane (APTES) were from J&K Scientific Ltd., China. Tris-(hydroxymethyl)aminomethane (Tris), polyethylene glycol-400 (PEG-400), acetic anhydride, and other general chemicals were from Dieckmann Co. Ltd., China. Solvents for synthesis were of analytical grade unless specified otherwise. Glass substrates for enzyme immobilization were from Sail Brand, China. UV-vis spectrophotometry was conducted on a NanoDrop One C spectrophotometer, Thermo Fisher Scientific, USA.

Immobilization of Enzymes on Glass Substrates.

There were two types of glass substrates for the immobilization of enzymes, planar glass slides and glass slides with a circular concave indentation of 1 cm in diameter and 1 mm in depth. Both types of glass slides were immersed in piranha solution, sonicated for 1 h, and rinsed with deionized water for several times followed by immersion into APTES in acetone for 3 h. The resulting APTES-treated glass slides were thoroughly washed with acetone and dried under a gentle flow of N_2 .

PEG-400 (0.5 g) and acetic anhydride (0.4 g) were stirred in 15 mL of DMSO at room temperature for 30 h. The resulting mixture was dialyzed against deionized water for 24 h, followed by freeze-drying to afford 0.3 g 1%-PEG-aldehyde (yield 60%).

Sodium alginate (10 g) was suspended in 100 mL of absolute ethanol followed by the addition of 10 mL of aqueous solution of NaIO_4 (1 g) and stirring for overnight at room temperature. The resulting partially oxidized alginate was collected by filtration, washed by absolute ethanol, and dialyzed against deionized water for 24 h followed by lyophilization to afford 6 g of pale-yellow solid.

A piece of APTES-treated planar glass slide was covered with a 0.1 M Tris-HCl buffer (pH 8.4) of the partially oxidized sodium alginate (1%) at room temperature for 6 h, followed by washing with deionized water. The slide was covered by PBS containing 1.0 mg mL^{-1} of collagenase for 3 h at room temperature, then washed with PBS buffer solution and immersed in a 1% NaBH_3CN solution at room temperature for 30 min. The collagenase-modified slide was kept at 4 °C before use.

A 1% PEG-aldehyde solution (in 0.1 M Tris-HCl, pH 8.4) was dropped onto and filled the cavity well of another piece of APTES-treated glass slide. The slide was allowed to stand at 37 °C for 6 h, followed by washing with deionized water. A 0.2% peptide solution in 0.1 M Tris-HCl buffer (pH 8.4) was then dropped onto and filled the indentation of the slide. It was allowed to stand at room temperature for 4 h. After washing

with deionized water, another portion of 1% PEG-aldehyde solution was used to fill the indentation for 6 h at 37 °C, followed by thorough washing by deionized water. The resulting indentation area of the slide modified by the response-linkers was filled with a PBS buffer solution (pH 7.4) containing 1.0 mg mL^{-1} of alginate lyase and HRP for 3 h at room temperature, washed with PBS buffer solution, and immersed in a 1% NaBH_3CN solution at room temperature for 30 min. The alginate lyase- and HRP-immobilized slide was kept at 4 °C before use.

Bacterial Culture. *P. aeruginosa*, *S. aureus*, *E. coli*, *S. enterica*, and *S. marcescens* were all obtained from ATCC and maintained in LB broth at 37 °C with constant shaking at 150 rpm. The number of bacteria in the original cultural media was determined by their optical density at 600 nm (OD600).

Assembly of the Biosensor and Biosensing Procedure. In a typical biosensing assay, the concave indentation of the slide immobilized with alginate lyase and HRP by the response-linkers was filled with 30 μL of the sample solution. The planar slide with collagenase immobilized by the looping-linkers was placed on the top to cover it. The assembly was kept at 25 °C for 15 min. The upper planar slide was then removed, and 10 μL of the aliquot in the lower concave indentation was transferred to one of the wells in a 96-well microplate. The TMB substrate (10 μL) was added to the well followed by incubation at 37 °C for 10 min. The oxTMB produced was transformed to a stable yellow color product by acidification with 2 μL of 2 M HCl and was monitored at 450 nm by a NanoDrop spectrophotometer.

Gelatin Zymography. Gelatin zymography was carried out following the literature procedure.⁴⁴ Images of PAGE gels were recorded by a Bio-Rad ChemiDoc Touch System.

Data Analysis. Unless otherwise stated, all experiments were performed in triplicate. Data presented are the averages + standard deviations of the results of the repeats. Data were analyzed by Student's *t*-test, and significant differences ($p < 0.01$ or 0.05 as reported in figure legends) are indicated by the asterisk symbol.

ASSOCIATED CONTENT

Supporting Information

The Supporting Information is available free of charge at <https://pubs.acs.org/doi/10.1021/acsomega.3c03533>.

Simulation of the enzyme kinetics of the AMELIE process (PDF)

AUTHOR INFORMATION

Corresponding Authors

Michael H. W. Lam – Department of Chemistry, City University of Hong Kong, Kowloon, Hong Kong;
Email: bhmhwlam@gmail.com

Yun Wah Lam – Department of Chemistry, City University of Hong Kong, Kowloon, Hong Kong; School of Applied Sciences, University of Huddersfield, Huddersfield HD1 3DH, U.K.; orcid.org/0000-0001-8929-5965; Email: y.lam@hud.ac.uk

Authors

Chuanwen Zhou – Department of Chemistry, City University of Hong Kong, Kowloon, Hong Kong

Xiaomin Li – Department of Chemistry, City University of Hong Kong, Kowloon, Hong Kong

Sze Wing Tang – Department of Chemistry, City University of Hong Kong, Kowloon, Hong Kong
Chunxi Liu – Department of Chemistry, City University of Hong Kong, Kowloon, Hong Kong

Complete contact information is available at:
<https://pubs.acs.org/10.1021/acsomega.3c03533>

Author Contributions

The manuscript was written through contributions of all authors. All authors have given approval to the final version of the manuscript.

Notes

The authors declare no competing financial interest.

ACKNOWLEDGMENTS

Funding from the Applied Research grant number 9667216 of City University of Hong Kong is acknowledged.

REFERENCES

- (1) Wang, B.; Anslyn, E. V. *Chemosensors: Principles, Strategies and Applications*; John Wiley & Sons, Inc.: Hoboken, New Jersey, 2011.
- (2) Zhou, X.; Lee, S.; Xu, Z.; Yoon, J. Recent progress on the development of chemosensors for gases. *Chem. Rev.* **2015**, *115*, 7944–8000.
- (3) Singh, K.; Rotaru, A. M.; Beharry, A. A. Fluorescent chemosensors as future tools for cancer biology. *ACS Chem. Biol.* **2018**, *13*, 1785–1798.
- (4) Mayer, M.; Baumner, A. J. A megatrend challenging analytical chemistry: biosensor and chemosensor concepts ready for the internet of things. *Chem. Rev.* **2019**, *119*, 7996–8027.
- (5) Serimin, P.; Prins, L. J. Sensing through signal amplification. *Chem. Soc. Rev.* **2011**, *40*, 4488–4505.
- (6) Crowther, J. R. *ELISA: Theory and Practice*; Humana Press: Totowa, NJ, 1995.
- (7) Gartner, Z. J.; Tse, B. N.; Grubina, R.; Doyon, J. B.; Snyder, T. M.; Liu, D. R. DNA-Templated Organic Synthesis and Selection of a Library of Macrocycles. *Science* **2004**, *305*, 1601–1605.
- (8) Shibata, A.; Uzawa, T.; Nakashima, Y.; Ito, M.; Nakano, Y.; Shuto, S.; Ito, Y.; Abe, H. Very rapid DNA-templated reaction for efficient signal amplification and its steady-state kinetic analysis of the turnover cycle. *J. Am. Chem. Soc.* **2013**, *135*, 14172–14178.
- (9) Nie, J.; Zhao, M. Z.; Xie, W. J.; Cai, L. Y.; Zhou, Y. L.; Zhang, X. X. DNA cross-triggered cascading self-amplification artificial biochemical circuit. *Chem. Sci.* **2015**, *6*, 1225–1229.
- (10) Jin, L. Y.; Dong, Y. M.; Wu, X. M.; Cao, G. X.; Wang, G. L. Versatile and amplified biosensing through enzymatic cascade reaction by coupling alkaline phosphatase in situ generation of photoresponsive nanozyme. *Anal. Chem.* **2015**, *87*, 10429–10436.
- (11) Berninger, T.; Bliem, C.; Piccinini, E.; Azzaroni, O.; Knoll, W. Cascading reaction of arginase and urease on a graphene-based FET for ultrasensitive, real-time detection of arginine. *Biosens. Bioelectron.* **2018**, *115*, 104–110.
- (12) Gianneschi, N. C.; Nguyen, S. T.; Mirkin, C. A. Signal amplification and detection via a supramolecular allosteric catalyst. *J. Am. Chem. Soc.* **2005**, *127*, 1644–1645.
- (13) Song, F.; Garner, A. L.; Koide, K. A highly sensitive fluorescent sensor for palladium based on the allylic oxidative insertion mechanism. *J. Am. Chem. Soc.* **2007**, *129*, 12354–12355.
- (14) Miranda, O. R.; Chen, H. T.; You, C. C.; Mortenson, D. E.; Yang, X. C.; Bunz, U. H. F.; Rotello, V. M. Enzyme-amplified array sensing of proteins in solution and in biofluids. *J. Am. Chem. Soc.* **2010**, *132*, 5285–5289.
- (15) Bonomi, R.; Cazzolaro, A.; Sansone, A.; Scrimin, P.; Prins, L. J. Detection of enzyme activity through catalytic signal amplification with functionalized gold nanoparticles. *Angew. Chem., Int. Ed.* **2011**, *50*, 2307–2312.
- (16) Munge, B. S.; Coffey, A. L.; Doucette, J. M.; Somba, B. K.; Malhotra, R.; Patel, V.; Gutkind, J. S.; Rusling, J. F. Nanostructured immunosensor for attomolar detection of cancer biomarker interleukin-8 using massively labeled superparamagnetic particles. *Am. Ethnol.* **2011**, *123*, 8061–8064.
- (17) Lei, J.; Ju, H. Signal amplification using functional nanomaterials for biosensing. *Chem. Soc. Rev.* **2012**, *41*, 2122–2134.
- (18) Roth, M. E.; Green, O.; Gnaim, S.; Shabat, D. Dendritic, oligomeric, and polymeric self-immolative molecular amplification. *Chem. Rev.* **2016**, *116*, 1309–1352.
- (19) Sun, X.; Reuther, J. F.; Phillips, S. T.; Anslyn, E. V. Coupling Activity-Based Detection, Target Amplification, Colorimetric and Fluorometric Signal Amplification, for Quantitative Chemosensing of Fluoride Generated from Nerve Agents. *Chem. – Eur. J.* **2017**, *23*, 3903–3909.
- (20) Kessenbrock, K.; Plaks, V.; Werb, Z. Matrix Metalloproteinases: Regulators of the Tumor Microenvironment. *Cell* **2010**, *141*, 52–67.
- (21) Caley, M. P.; Martins, V. L. C.; O’Toole, E. A. Metalloproteinases and wound healing. *Adv. Wound Care* **2015**, *4*, 225–234.
- (22) Soria-Valles, C.; Gutiérrez-Fernández, A.; Osorio, F. G.; Carrero, D.; Ferrando, A. A.; Colado, E.; Fernández-García, M. S.; Bonzon-Kulichenko, E.; Vázquez, J.; Fueyo, A.; López-Otín, C. MMP-25 Metalloprotease Regulates Innate Immune Response through NF- κ B Signaling. *J. Immunol.* **2016**, *197*, 296–302.
- (23) Tomlin, H.; Piccinini, A. M. A Complex Interplay between the DNA Damage Response and the Immunological Landscape Shaping the Tumor Microenvironment. *Immunology* **2018**, *155*, 186–201.
- (24) Chitlaru, T.; Gat, O.; Gozian, Y.; Ariel, N.; Shafferman, A. Differential proteomic analysis of the *Bacillus anthracis* secretome: distinct plasmid and chromosome CO₂-dependent cross talk mechanisms modulate extracellular proteolytic activities. *J. Bacteriol.* **2006**, *188*, 3551–3571.
- (25) Zou, H.-S.; Song, X.; Zou, L.-F.; Yuan, L.; Li, Y.-R.; Guo, W.; Che, Y.-Z.; Zhao, W.-X.; Duan, Y.-P.; Chen, G.-Y. EcpA, an extracellular protease, is a specific virulence factor required by *Xanthomonas oryzae* pv. *oryzicola* but not by *X. oryzae* pv. *oryzae* in rice. *Microbiology* **2012**, *158*, 2372–2383.
- (26) Mukherji, R.; Patil, A.; Prabhune, A. Role of Extracellular Proteases in Biofilm Disruption of Gram Positive Bacteria with Special Emphasis on *Staphylococcus aureus* Biofilms. *Enzyme Eng.* **2014**, *4*, 126.
- (27) Vanlaere, C.; Libert, C. Matrix metalloproteinases as drug targets in infections caused by gram-negative bacteria and in septic shock. *Clin. Microbiol. Rev.* **2009**, *22*, 224–239.
- (28) Patel, S.; Sumitra, G.; Koner, B. C.; Saxena, A. Role of serum matrix metalloproteinase-2 and-9 to predict breast cancer progression. *Clin. Biochem.* **2011**, *44*, 869–872.
- (29) Cathcart, A.; Pulkoski-Gross, A.; Cao, J. Targeting matrix metalloproteinases in cancer: bringing new life to old ideas. *Genes Dis.* **2015**, *2*, 26–34.
- (30) Khalid, M. A.; Javaid, M. A. Matrix metalloproteinases: new targets in cancer therapy. *J. Cancer Sci. Ther.* **2016**, *8*, 143–153.
- (31) Kupai, K.; Szucs, G.; Cseh, S.; Hajdu, I.; Csonka, C.; Csont, T.; Ferdinandy, P. Matrix Metalloproteinase Activity Assays: Importance of Zymography. *J. Pharmacol. Toxicol. Methods* **2010**, *61*, 205–209.
- (32) Tajhya, R. B.; Patel, R. S.; Beeton, C. Detection of matrix metalloproteinases by zymography. *Matrix Metalloproteinases: Methods and Protocols* **2017**, 231–244.
- (33) Zayats, M.; Raitman, O. A.; Chegel, V. I.; Kharitonov, A. B.; Willner, I. Probing antigen–antibody binding processes by impedance measurements on ion-sensitive field-effect transistor devices and complementary surface plasmon resonance analyses: Development of cholera toxin sensors. *Anal. Chem.* **2002**, *74*, 4763–4773.
- (34) Lin, J.; Wang, J.; Wang, T.; Li, D.; Xi, F.; Wang, J.; Wang, E. Three-dimensional electrochemical immunosensor for sensitive detection of carcinoembryonic antigen based on monolithic and macroporous graphene foam. *Biosens. Bioelectron.* **2015**, *65*, 281–286.

- (35) Li, S.-Y.; Liu, L.-H.; Cheng, H.; Li, B.; Qiu, W.-X.; Zhang, X.-Z. A dual-FRET-based fluorescence probe for the sequential detection of MMP-2 and caspase-3. *Chem. Commun.* **2015**, *51*, 14520–14523.
- (36) Jing, P.; Yi, H.; Xue, S.; Yuan, R.; Xu, W. A 'signal on-off' electrochemical peptide biosensor for matrix metalloproteinase 2 based on target induced cleavage of a peptide. *RSC Adv.* **2015**, *5*, 65725–65730.
- (37) Meng, F.; Sun, H.; Huang, Y.; Tang, Y.; Chen, Q.; Niao, P. Peptide cleavage-based electrochemical biosensor coupling graphene oxide and silver nanoparticles. *Anal. Chim. Acta* **2019**, *1047*, 45–51.
- (38) Xiong, E.; Zhang, X.; Liu, Y.; Zhou, J.; Yu, P.; Li, X.; Chen, J. Ultrasensitive electrochemical detection of nucleic acids based on the dual-signaling electrochemical ratiometric method and exonuclease III-assisted target recycling amplification strategy. *Anal. Chem.* **2015**, *87*, 7291–7296.
- (39) Wang, D.; Yuan, Y.; Zheng, Y.; Chai, Y.; Yuan, R. An electrochemical peptide cleavage-based biosensor for matrix metalloproteinase-2 detection with exonuclease III-assisted cycling signal amplification. *Chem. Commun.* **2016**, *52*, 5943–5945.
- (40) Yoon, H. K.; Jung, S. T.; Kim, J. H.; Yoo, T. H. Recent development of highly sensitive protease assay methods: Signal amplification through enzyme cascades. *Biotechnol. Bioprocess Eng.* **2012**, *17*, 1113–1119.
- (41) Stein, V.; Alexandrov, K. Protease-based synthetic sensing and signal amplification. *Proc. Natl. Acad. Sci.* **2014**, *111*, 15934–15939.
- (42) Kim, H.; Yoon, H. K.; Yoo, T. H. Engineering β -lactamase zymogens for use in protease activity assays. *Chem. Commun.* **2014**, *50*, 10155–10157.
- (43) Sun, X.; Shabat, D.; Phillips, S. T.; Anslyn, E. V. Self-propagating amplification reactions for molecular detection and signal amplification: Advantages, pitfalls, and challenges. *J. Phys. Org. Chem.* **2018**, *31*, No. e3827.
- (44) Toth, M.; Sohail, A.; Fridman, R. Assessment of Gelatinases (MMP-2 and MMP-9) by Gelatin Zymography. In *Metastasis Research Protocols*; Dwek, M., Brooks, S., Schumacher, U., Eds.; Humana Press: Totowa, NJ, 2012; Vol. 878, DOI: 10.1007/978-1-61779-854-2_8.
- (45) West, J. L.; Hubbell, J. A. Polymeric biomaterials with degradation sites for proteases involved in cell migration. *Macromolecules* **1999**, *32*, 241–244.
- (46) Lee, S. H.; Moon, J. J.; Miller, J. S.; West, J. L. Poly (ethylene glycol) hydrogels conjugated with a collagenase-sensitive fluorogenic substrate to visualize collagenase activity during three-dimensional cell migration. *Biomaterials* **2007**, *28*, 3163–3170.
- (47) Harris, J. M.; Struck, E. C.; Case, M. G.; Yalpani, M.; Van Alstine, J. M.; Brooks, D. E. Synthesis and characterization of poly (ethylene glycol) derivatives. *J. Polym. Sci. Polym. Chem. Ed.* **1984**, *22*, 341–352.
- (48) Veronese, F. M. Peptide and protein PEGylation: a review of problems and solutions. *Biomaterials* **2001**, *22*, 405–417.
- (49) Yu, W.; Gu, N.; Zhang, H.-Q.; Wu, J.-G.; Wang, Y.-H.; Wesche, K.-D. Microarray preparation based on oxidation of agarose-gel and subsequent enzyme immunoassay. *Sens. Actuators, B* **2004**, *98*, 83–91.
- (50) Gutiérrez, O. A.; Salas, E.; Hernández, Y.; Lissi, E. A.; Castrillo, G.; Reyes, O.; Garay, H.; Aguilar, A.; García, B.; Otero, A.; Chavez, M. A.; Duarte, C. A. An immunoenzymatic solid-phase assay for quantitative determination of HIV-1 protease activity. *Anal. Biochem.* **2002**, *307*, 18–24.
- (51) Gutiérrez, O. A.; Chavez, M.; Lissi, E. A theoretical approach to some analytical properties of heterogeneous enzymatic assays. *Anal. Chem.* **2004**, *76*, 2664–2668.
- (52) Watanabe, K. Collagenolytic proteases from bacteria. *Appl. Microbiol. Biotechnol.* **2004**, *63*, 520–526.
- (53) Shaw, L.; Golonka, E.; Potempa, J.; Foster, S. J. The role and regulation of the extracellular proteases of *Staphylococcus aureus*. *Microbiology* **2004**, *150*, 217–228.
- (54) Frees, D.; Brøndsted, L.; Ingmer, H. Bacterial Proteases and Virulence. In: Dougan, D. (Ed.), *Regulated Proteolysis in Microorganisms. Subcellular Biochemistry*, Vol. 66, Springer, Dordrecht, 2013, pp. 161–182.
- (55) Iseri, E.; Biggel, M.; Goossens, H.; Moons, P.; van der Wijngaert, W. Digital dipstick: miniaturized bacteria detection and digital quantification for the point-of-care. *Lab Chip* **2020**, *20*, 4349–4356.
- (56) Klisara, N.; Yu, Y. M.; Palaniappan, A.; Liedberg, B. Towards on-site visual detection of proteases in food matrices. *Anal. Chim. Acta* **2019**, *1078*, 182–188.
- (57) Buss, C. G.; Dudani, J. S.; Akana, R. T.; Fleming, H. E.; Bhatia, S. N. Protease activity sensors noninvasively classify bacterial infections and antibiotic responses. *EBioMedicine* **2018**, *38*, 248–256.
- (58) Rawlings, N. D.; Bateman, A. How to use the MEROPS database and website to help understand peptidase specificity. *Protein Sci.* **2021**, *30*, 83–92.